Contents lists available at ScienceDirect

Journal of Environmental Management

journal homepage: http://ees.elsevier.com

Modeling the impact of the COVID-19 lockdowns on urban surface ecological status: A case study of Milan and Wuhan cities

Mohammad Karimi Firozjaei [a], Solmaz Fathololomi [b], Majid Kiavarz [a,*], Jamal Jokar Arsanjani [c], Mehdi Homaee[d,1], Seyed Kazem Alavipanah [a]

[a] Department of Remote Sensing and GIS, Faculty of Geography, University of Tehran, Tehran, Iran
[b] Faculty of Agriculture and Natural Resources, University of Mohaghegh Ardabili, Ardabil, Iran
[c] Geoinformatics Research Group, Department of Planning and Development, Aalborg University Copenhagen, A.C. Meyers Vænge 15, DK-2450, Copenhagen, Denmark
[d] Agrohydrology Research Group, College of Agriculture, Tarbiat Modares University, Tehran 14115-336, Iran.

ARTICLE INFO

Keywords
Environment
Lockdown
Comprehensive ecological evaluation index
Anthropogenic activities
Remote sensing

ABSTRACT

The COVID-19 pandemic has caused unprecedent negative impacts on our society, however, evidences show a reduction of anthropogenic pressures on the environment. Due to the high importance of environmental conditions on human life quality, it is crucial to model the impact of COVID-19 lockdown on environmental conditions. Consequently, the objective of this study was to model the impact of COVID-19 lockdown on the urban surface ecological status (USES). To this end, the Landsat-8 images of Milan for three pre-lockdown dates (Feb 13, 2018 (MD1), April 18, 2018 (MD2) and Feb 3, 2020 (MD3)) and one date over the lockdown (April 14, 2020 (MD4)), and Wuhan for three pre-lockdown dates (Dec 17, 2017 (WD1), March 23, 2018 (WD2) and Dec 7, 2019 (WD3)) and one lockdown date (Feb 9, 2020 (WD4)) were used. First, pressure-state-response (PSR) framework parameters including index-based built-up index (IBI), vegetation cover (VC), vegetation health index (VHI), land surface temperature (LST) and Wetness were calculated. Second, by combining the PSR framework parameters based on comprehensive ecological evaluation index (CEEI), the USES were modeled on different dates. Thirdly, the USES during the COVID-19 lockdown was compared with the USES for pre-lockdown. The mean (standard deviation) of CEEI for Milan on MD1, MD2, MD3 and MD4 were 0.52 (0.12), 0.60 (0.19), 0.57 (0.13) and 0.45 (0.16), respectively. Also, these values for Wuhan on WD1, WD2, WD3 and WD4 were 0.63 (0.14), 0.67 (0.15), 0.60 (0.13) and 0.57 (0.13), respectively. Due to the lockdowns, the mean CEEI of built-up, bare soil and green spaces for Milan and Wuhan decreased by [0.18, 0.02, 0.08], [0.13, 0.06, 0.05], respectively. During the lockdown period, the USES improved substantially due to the reduction of anthropogenic activities in the urban environment.

1. Introduction

Coronavirus disease, also known as COVID-19, is an infectious disease caused by the coronavirus Acute Respiratory Syndrome (SARS-CoV-2) (Lai et al., 2020). The disease was first reported in Wuhan, China on December 31, 2019, and outbroke rapidly around the world due to its contagious nature in a way that involved all countries of the world (Qin et al., 2020). COVID-19 was recognized as an epidemic on January 2020 (Velavan and Meyer, 2020). Nearly 61 million people in the world are infected by the disease until November 25, 2020, of whom 1,420,000 persons have died (WHO, 2020). Due to the huge impact of COVID-19 on people's health and with the increase in the number of cases of this disease, most countries have introduced special and preventive rules and proceedings for social interactions in order to prevent the spread of the virus (Lau et al., 2020). These special and deterrent proceedings include enforcing social/physical distancing recommendations, banning public events, closing schools, universities and unnecessary jobs, closing counties, borders, and dramatically reducing train, bus, and air travels (Gao et al., 2020; Nicola et al., 2020). Lockdown regulations were also reinforced in many global large cities (Mahato et al., 2020; Muhammad et al., 2020; Nakada and Urban, 2020).

The prevalence of COVID-19 and the implemented lockdowns around the world have had a significant negative impact on the global economy. However, the environment has been relieved of the pressures of anthropogenic activities on a local, regional and global scales (Chakraborty and Maity, 2020; Muhammad et al., 2020; Nakada and Urban, 2020; Zambrano-Monserrate et al., 2020). Due to the high importance of environmental conditions on human life quality (Firozjaei et al., 2020c), it is of outmost important to model the impact of COVID-19 lockdown on environmental conditions (Berman and Ebisu, 2020; Nakada and Urban, 2020).

* Corresponding author.
E-mail addresses: mohammad.karimi.f@ut.ac.ir (M.K. Firozjaei); fathis@uma.ac.ir (S. Fathololomi); kiavarzmajid@ut.ac.ir (M. Kiavarz); jja@plan.aau.dk (J.J. Arsanjani); mhomaee@modares.ac.ir (M. Homaee); salavipa@ut.ac.ir (S.K. Alavipanah)
[1] Department of Mining Engineering, Faculty of Engineering, Tarbiat Modares University, Tehran 14115, Iran

https://doi.org/10.1016/j.jenvman.2021.112236
Received 26 July 2020; Received in revised form 16 February 2021; Accepted 18 February 2021

Recent studies used earth observation data to model the impact of COVID-19 lockdown on environmental conditions, for instance, Tobías et al. (2020) evaluated air pollution changes in Barcelona during lockdown. The results showed that during the lockdown, air pollution in Barcelona, especially traffic-related pollutants such as carbon black and NO_2, was significantly reduced. Nakada and Urban (2020) examined the impact of COVID19 lockdown on air quality in Sao Paulo, Brazil. The results showed that the amount of NO, NO_2 and CO in the air of this state decreased by 70, 54.3 and 64.8%, respectively during the lockdown period compared to the pre-lockdown period, however, the concentration of Ozone in this area increased by 30% for the same period due to a significant reduction in carbon monoxide. Mandal and Pal (2020) examined the effects of lockdown on various aspects of the environmental conditions of an area in eastern India, including noise, particulate matter (PM_{10}), land surface temperature (LST) and river water quality. The results show that the maximum concentration of PM_{10} from 189 to 278 μg/m^3 in the pre-lockdown period reached to 50–60 μg/m^3 in the lockdown period. The LST reduced by 3–5°, noise levels also decreased from 85 dBA to 85 dBA along with improvement of river water quality.

The results of these studies showed that due to the complete cessation of industrial, transportation and tourism sectors and a significant reduction in population accumulation in public spaces during the COVID-19 lockdown, the adverse effects of these activities on the environment have been substantial reduced.

The urban surface ecological status (USES) indicate the urban environmental conditions and is one of the factors affecting the human life's quality. Consequently, it is crucial to model the spatial and temporal changes of USES. This parameter is a function of the parameters related to the pressure-state-response (PSR) framework. The components of this framework include climate responses, environmental states and anthropogenic pressures. The purpose of this study is to model the impact of COVID-19 lockdown on the USES.

The remainder of this paper is structured as follows, section 2 presents the study area and section 3 presents the data and methods used in the study. Section 4 presents the results followed by discussions in section 5 summing up with conclusions in section 6.

2. Study area

To evaluate the impact of COVID-19 lockdown on the USES, Milan and Wuhan cities as two hot spots of outbreak were selected as study areas (Fig. 1). COVID-19 had a significant impact on the conditions of Milan and Wuhan cities among other cities in the world. The prevalence of COVID-19 seemed to start from Wuhan. By November 25, 2020, more than 148,000 and 50,340 people were infected by this disease in Milan and Wuhan cities, respectively. The number of deaths due to COVID-19 in these cities were 10,765 and 3869 people as of November 12, 2020, respectively (WHO, 2020). The COVID-19 lockdown dates was from Mar 10, 2020 to Apr 8, 2020 for Milan city and Jan 23, 2020 to Apr 8, 2020 for Wuhan city.

Milan is located in 9° 5′ 51′′ to 9° 16′ 44′′ E longitude and from 45° 25′ 42′′ to 45° 32′ 10′′ N latitude in the north of Italy, which is the second most populous city in Italy with a population of more than 1.4 million. This city is of great economic and cultural importance. Milan city has hot and humid summers and cold and foggy winters. The mean elevation of this city is 120 m above sea level.

Wuhan is located in 114° 3′ 40′′ to 114° 32′ 58′′ E longitude and from 30° 28′ 8′′ to 30° 46′ 38′′ N latitude of China. With a population of over 11 million, it is one of the most populous, political, economic, financial, commercial, cultural and educational city in central China. Wuhan has relatively cold winters and hot and rainy summers.

3. Data and methods

3.1. Data

To extract surface characteristics including different spectral indices and land cover maps, and to model the impact of COVID-19 lockdown on USES, Landsat-8 reflective and thermal bands were used. For each of the cities, 4 Landsat-8 images from different dates were selected. These images include one suitable image during the lockdown period (April 14, 2020 (MD4) for Milan and Feb 9, 2020 (WD4) for Wuhan), one suitable image at the closest possible date before the start of the lockdown (Feb 3, 2020 (MD3) for Milan and Dec 7,

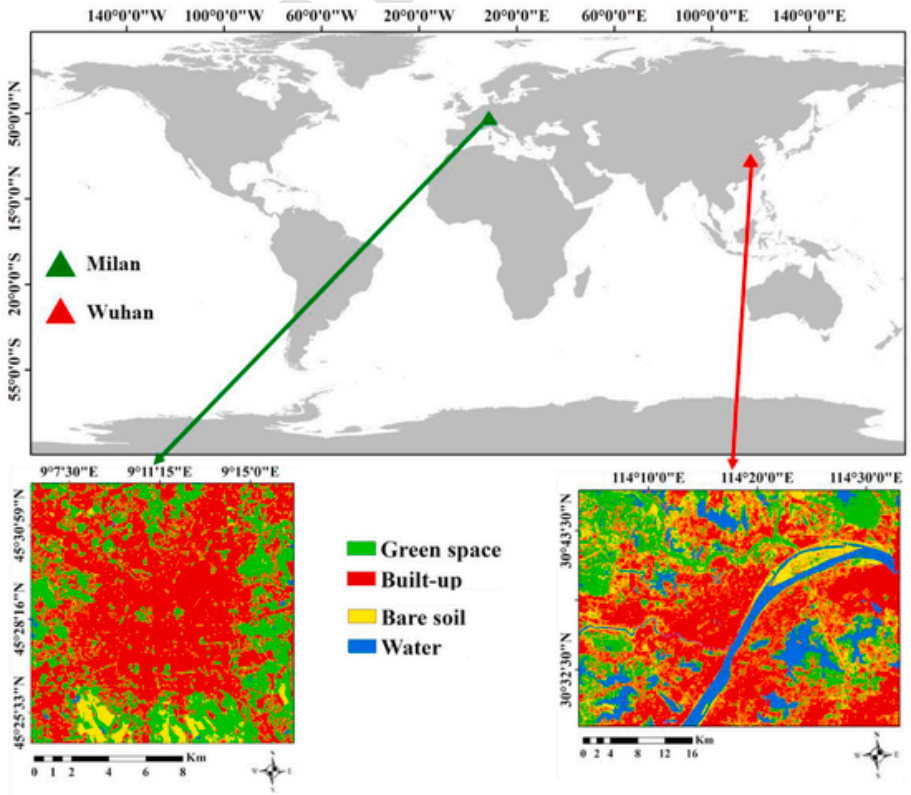

Fig. 1. Geographical location of study area and their land cover information.

2019 (WD3) for Wuhan) and two suitable images in the closest possible dates to the first two images in previous years (Apr 18, 2018 (MD2) and Feb 13, 2018 (MD1) for Milan and Mar 23, 2018 WD2) and Dec 17, 2017 (WD1) for Wuhan). Images were selected based on time conditions relative to the lockdown date of each city and cloud cover less than 10%. Moreover, weather conditions have been considered in the dates, and for at least 4 days before the selected dates, there was no rainfall in the studied cities. Row and Path specifications of these images are 29 and 193 for Milan city and 39 and 123 for Wuhan city, respectively. The characteristics of Landsat-8 images are provided in Weng et al. (2019). Google Earth images were used to extract training-testing datasets for land cover classification. Daily water vapor (MOD07) and surface temperature products (MOD11A1) were also used to calculate the LST obtained from the Landsat-8 reflective and thermal bands.

3.2. Methods

The schematic flowchart shown in Fig. 2 was used to model and evaluate the impact of COVID-19 lockdown on the USES. In the first step, the parameters related to the PSR framework including index-based built-up index (IBI), vegetation cover (VC), vegetation health index (VHI), LST and Wetness were calculated based on the combination of Landsat-8 reflective and thermal bands at different dates. In the second step, by combining the information of PSR framework parameters based on CEEI, the USES were modeled at different dates. In the third step, the USES during the COVID-19 lockdown period were compared against the USES in the pre-lockdown period.

3.2.1. PSR framework parameters

The used spectral indices and methods to extract the PSR framework parameters are presented in Table 1. Normalized difference vegetation index (NDVI) is one of the most widely used index in assessment and modeling of vegetation (Robinson et al., 2017). VC can show vegetation fraction in one pixel in the range of 0–1 values indicating pixels with least vegetation cover i.e., totally impervious or soil surface to pixels with most vegetation cover i.e., totally vegetation, respectively (Sobrino et al., 2008). VC can easily demonstrate the vegetation fraction in one pixel; however, not ideal for indicating vegetation health. Hence, VHI was used to tackle this challenge, since it considers the levels of chlorophyll, nitrogen and xanthophyll for quantifying vegetation health (Yang et al., 2020). Consequently, in order to consider each of these characteristics, NDVI, nitrogen reflectance index (NRI), and normalized difference senescent vegetative index (NDSVI), which represent chlorophyll, nitrogen, and xanthophyll were combined using Principal Component Analysis (PCA) and consequently VHI was calculated (Yang et al., 2020). Studies show that IBI is highly effective in showing the percentage of impervious surface cover in a pixel. A pixel with a higher IBI value contains a higher fraction of built-up (Hu and Xu, 2018; Xu, 2008). Wetness can indicate the amount of moisture in the surface of various covers including built-up, bare soil and vegetation covers. The use of tasseled cap transformation (TCT) is one of the most common methods for modeling spatial heterogeneity of wetness (Baig et al., 2014). LST is one of the most important surface physical properties that can indicate the exchange of thermal energy between the subsurface, surface and the atmosphere (Jiménez-Muñoz et al., 2014; Weng et al., 2019). Studies have shown that increasing human activity in an area increases LST (Firozjaei et al., 2018, 2020d; Xiao and Weng, 2007). Also, spatial and

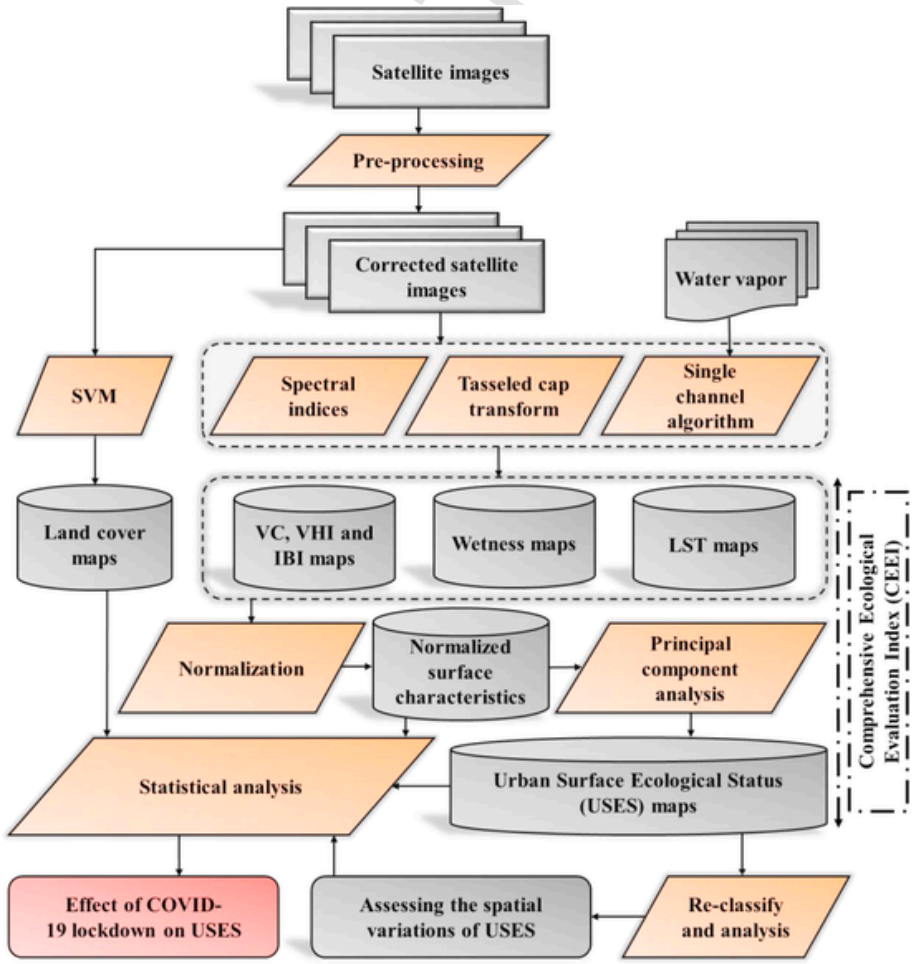

Fig. 2. Schematic flowchart of the conducted study.

Table 1
The spectral indices and methods used for modeling PSR framework parameters.

Parameters	PSR framework	Equation	References
IBI	Pressure intensity	$\left(\left(\frac{2SWIR1}{SWIR1+NIR}\right)-\left(\frac{NIR}{NIR+Red}\right)+\left(\frac{Green}{Green+SWIR1}\right)\right)/\left(\left(\frac{2SWIR1}{SWIR1+NIR}\right)+\left(\frac{NIR}{NIR+Red}\right)-\left(\frac{Green}{Green+SWIR1}\right)\right)$	(Hu and Xu, 2018; Xu, 2008)
NDVI	Environmental states	$\frac{NIR-Red}{NIR+Red}$	Sobrino et al. (2008)
VC		$\frac{(NDVI-NDVI_{soil})}{(NDVI_{Veg}-NDVI_{soil})}$	
NRI		$\frac{NIR}{Green}$	Yang et al. (2020)
NDSVI		$\frac{SWIR1-Green}{SWIR1+Green}$	
VHI		$PCA\,(NDVI,\ NRI,\ NDSVI)$	
		$\frac{(PC1-PC1_{min})}{(PC1_{max}-PC1_{min})}$	
Wetness	Climate responses	$0.1115Blue2-0.1973Green+0.3283Red+0.3407NIR-0.7117SWIR1-0.4559SWIR2$	Baig et al. (2014)
LST		$LST=\gamma\left(\frac{1}{LSE}\left(\psi_1 L_{sen}+\psi_2\right)+\psi_3\right)+\delta$	Jiménez-Muñoz et al. (2014)

temporal changes in LST can be a function of climatic conditions (Weng, 2009).

Information from at least two or more reflective and thermal bands of satellite images was used to calculate these parameters. The quick atmospheric correction (QUAC) model was used for atmospheric correction of Landsat-8 reflective bands. This model is straightforward and requires minimal inputs for atmospheric correction. The NDVI threshold method (Sobrino et al., 2008) was used to calculate the land surface emissivity in the LST calculation. In this study, the third component obtained from TCT was used to model the surface wetness properties.

The support vector machines (SVM) method was used to generate land cover maps (Foody and Mathur, 2004; Otukei and Blaschke, 2010). This method is one of the non-parametric and supervised classification methods. The main advantage of this method is its high ability to use less training samples and its reported higher accuracy compared to other methods. The main purpose of this algorithm is to find the maximum distance between two classes and thus increase the classification accuracy. In this study, the RBF kernel (With set 300 for C and 3 for γ) were used in the SVM model to classify land cover.

3.2.2. USES modeling

CEEI is one of the efficient methods for modeling USES (Yang et al., 2020). In this method, the PSR framework parameters (Hughey et al., 2004; Xu et al., 2019) is combined with each other using Eq. (1) to model the USES.

$$CEEI = PCA(Pressure\ intensity,\ Environmental\ states,\ Climate\ responses) \quad (1)$$

In equation (1), PC1 indicates the USES' spatial heterogeneity. The amount of anthropogenic activities in an area has a high correlation with the percentage of impervious surface covers. Consequently, IBI was used to consider pressure intensity. VC and VHI were used to consider environmental states that reflect cover and quality of vegetation. Finally, LST and Wetness were used to consider climate responses such as humidity and temperature conditions (Yang et al., 2020). Of course, pressure intensity on the environment caused by anthropogenic activities can also have a high correlation with LST.

To reduce the effects of seasonal changes and climatic conditions in modeling the trend of USES changes, each of the PSR framework parameters at different dates, was standardized into 0 and 1 based on the maximum and minimum values of each characteristic. According to the type of impact of each parameter on the USES, Eq. (2) was used for LST and IBI standardization and Eq. (3) was used for VC, VHI and Wetness standardization.

$$SX_i = \frac{(X_i - X_{min})}{(X_{max} - X_{min})} \quad (2)$$

$$SX_i = \frac{(X_{max} - X_i)}{(X_{max} - X_{min})} \quad (3)$$

In equations (2) and (3), SX_i was the values of the standardized parameters, X_i was the initial values of the parameters, and X_{min} and X_{max} were the lowest and highest parameter values in the area, respectively.

In this study, to quantify the USES, the standardized parameters related to the PSR framework have been used as Eq. (4).

$$CEEI = PC1\,(IBI,\ VC,\ VHI,\ LST,\ Wetness) \quad (4)$$

The CEEI value obtained from Eq. (4) is standardized into 0 and 1 using Eq. (2). Values of 1 and 0 for CEEI indicate the worst and best USES, respectively. Areas with maximum LST and IBI and minimum VC, VHI and Wetness have the worst USES and vice versa. Before the implementation of CEEI, water covers were masked based on the selection of an appropriate threshold of NDVI. CEEI values were classified into 5 levels of USES based on Table 2 (Hu and Xu, 2018; Xu et al., 2018; Yang et al., 2020).

3.2.3. Modeling the effect of the lockdowns on the USES

To investigate the impact of COVID-19 lockdown on the USES, the following steps were followed:

1. The mean and standard deviation (SD) of surface characteristics of Milan and Wuhan cities including heat (LST), greenness (NDVI), imperviousness and dryness surface (IBI) and wetness (Wetness) in COVID-19 lockdown date and pre-lockdown dates were calculated and compared against each other.
2. The mean and SD of the CEEI of Milan and Wuhan at the COVID-19 lockdown date and the pre-lockdown dates were calculated and compared.
3. The area of the different USES classes of Milan and Wuhan cities at the COVID-19 lockdown date and the pre-lockdown date was calculated and compared.
4. Based on Table 3, the type of change in the USES of Milan and Wuhan cities between the lockdown date and the pre-lockdown dates was deter-

Table 2
The USES classes based on CEEI.

CEEI ranges	USES classes	Descriptions
0.0–0.02	Excellent	These areas have excellent USES. Ecosystem performance is excellent. These areas have complete and healthy vegetation and there are no human activities in these areas
0.2–0.4	Very good	These areas have very good USES. Ecosystem performance is very good. These areas have a lot of healthy vegetation and human activities are very low in these areas.
0.4–0.6	Good	These areas have good USES. These areas have moderate vegetation and human activities in these areas are not much. The effect of urban heat island in these urban areas is not obvious.
0.6–0.8	Fair	These areas have fair USES. Ecosystem performance is not good, but it is a restoration function. These areas have poor vegetation and human activities in these areas are high. The effect of an urban thermal island is evident in these urban areas.
0.8–1.0	Poor	These areas have poor USES. Ecosystem performance is unfavorable. These areas lack vegetation and human activities in these areas are very high and the effect of urban heat island and drought in these urban areas is obvious.

mined. Then, the area of Improved, Unchanged and Degraded classes was calculated.

5. The mean CEEI of Milan and Wuhan cities at the lockdown date and the pre-lockdown dates were calculated for each land cover class and compared with each other.
6. The mean CEEI difference between the COVID-19 lockdown date and the pre-lockdown date was calculated and compared at the study area and each land cover scale.
7. The correlation coefficient (r) between the impervious surface degree (IBI) and the CEEI changes of Milan and Wuhan in the lockdown date and the pre-lockdown date was calculated and evaluated.

4. Results

The spatial distribution of surface characteristics of Milan and Wuhan cities in different dates was found heterogeneous as shown in Fig. 3. A visual examination of the surface characteristics maps shows that the amount of LST and IBI of the built-up lands was higher than the areas with other lands. Also, the amount of NDVI and Wetness of areas with built-up lands was less than other areas. The spatial and temporal variations of LST in both cities are greater than NDVI, IBI and Wetness. The biggest differences in surface characteristics patterns between built up and non-built up areas of Milan and Wuhan are for MD2 and WD2, respectively. The LST changes during COVID-19 lockdown (MD4 for Milan and WD4 for Wuhan) compared to the same dates in 2018 were more than other surface characteristics. Many areas with high LST values on MD2 (Milan) and WD2 (Wuhan) were changed to areas with medium and low LST values on MD4 (Milan) and WD4 (Wuhan). However, changes in other surface characteristics at these dates were not high relative to LST changes.

The mean and SD of the surface characteristics of these cities in different dates were different due to seasonal changes, land cover and human activities changes (Table 4). For Milan, the difference in SD of LST values for the dates MD4 (1.29 °C) and MD2 (2.21 °C) was greater than the dates MD3 (1.03 °C) and MD1 (0.89 °C). For Wuhan, the difference in SD values of LST for dates WD4 (2.02 °C) and WD2 (3.44 °C) was more than WD3 (1.63 °C) and WD1 (1.53 °C). COVID-19 lockdown has significantly reduced the spatial heterogeneity of LST in Milan and Wuhan cities. This result shows that the impact of human activities on the spatial distribution of surface characteristics can be greater than the impact of climatic and seasonal conditions. The impact of human activities on the spatial distribution of IBI and Wetness in Wuhan was greater than in Milan. The mean of NDVI and LST in Milan city was higher than in Wuhan city. For Milan city, the highest SD values were IBI, NDVI and Wetness on MD4. In general, the temporal changes in the surface characteristics of Milan city were more than Wuhan city.

The spatial distribution of CEEI values in Milan and Wuhan cities varies at different dates (Fig. 4). Urban areas with built-up land cover have the highest CEEI values due to the low values of greenness and wetness and high values of the impervious cover, dryness and heat. The USES of Milan city on MD1 worsened compared to MD2. Consequently, the ecological conditions of many areas with Good and Fair classes on MD1 were changed to Poor class on MD2. However, due to the COVID-19 lockdowns and the significant reduction of human activities, the ecological conditions of this city improved from MD3 to MD4. Ecological conditions of most parts of Milan city were changed from Fair and Good classes to Good and Very good classes. For Milan, the spatial similarity of CEEI values on MD3 and MD1 was higher than on MD4 and MD2. The correlation coefficient (r) between CEEI values on these dates were 0.76 and 0.63, respectively. For Wuhan, the changes in ecological conditions on WD1 compared to WD2 were more than the changes on WD3 compared to WD4. The r between CEEI values on WD1 and WD3 and on WD2 and WD4 was 0.88 and 0.79, respectively.

The mean (SD) of CEEI for Milan on MD1, MD2, MD3 and MD4 were 0.52 (0.12), 0.60 (0.19), 0.57 (0.13) and 0.45 (0.16), respectively. Also, these values for Wuhan on WD1, WD2, WD3 and WD4 were 0.63 (0.14), 0.67 (0.15), 0.60 (0.13) and 0.57 (0.13), respectively. In all dates, the best USES were related to the green space lands of Milan and Wuhan cities (Table 5). For the pre-lockdown dates, the worst USES was related to built-up lands in these cities, but in the lockdown date, the mean CEEI decreased and was lower than the mean CEEI of bare soil lands. The lowest and highest differences between the mean CEEI of built-up lands and green space lands were in the date of lockdown (MD4 for Milan and WD4 for Wuhan) and the similar dates in last year (MD2 for Milan and WD2 for Wuhan). In general, the results show that among the different dates, the best USES in Milan and Wuhan cities were on the lockdown dates.

The highest area of Excellent and Very good classes and the lowest area of Fair and Poor classes in both Milan and Wuhan cities were related to the COVID-19 lockdown date (Table 6). The results show that among the different dates, the best USES in Milan and Wuhan cities were related to the COVID-19 lockdown dates. However, the USES of these cities were bad on the same dates in previous years. The highest area of Poor class for Milan and Wuhan cities was related to MD2 and WD2 dates, respectively, due to the various factors such as climatic and seasonal conditions and human activities.

The USES of more than 70% of Milan city have improved on MD4 compared to MD2 (Table 7). Also, USES of only 2.5% of Milan have been destroyed on MD4 compared to MD3, while this amount was more than 45% on MD2 compared to MD1. For Wuhan the USES of more than 52% of this city on COVID-19 lockdown date (WD4) improved than USES on WD2. Conse-

Table 3
Type of change in USES classes between pre-lockdown date and lockdown dates.

	Lockdown date				
Pre-lockdown date	Excellent	Very good	Good	Fair	Poor
Excellent	Unchanged	Degraded	Degraded	Degraded	Degraded
Very good	Improved	Unchanged	Degraded	Degraded	Degraded
Good	Improved	Improved	Unchanged	Degraded	Degraded
Fair	Improved	Improved	Improved	Unchanged	Degraded
Poor	Improved	Improved	Improved	Improved	Unchanged

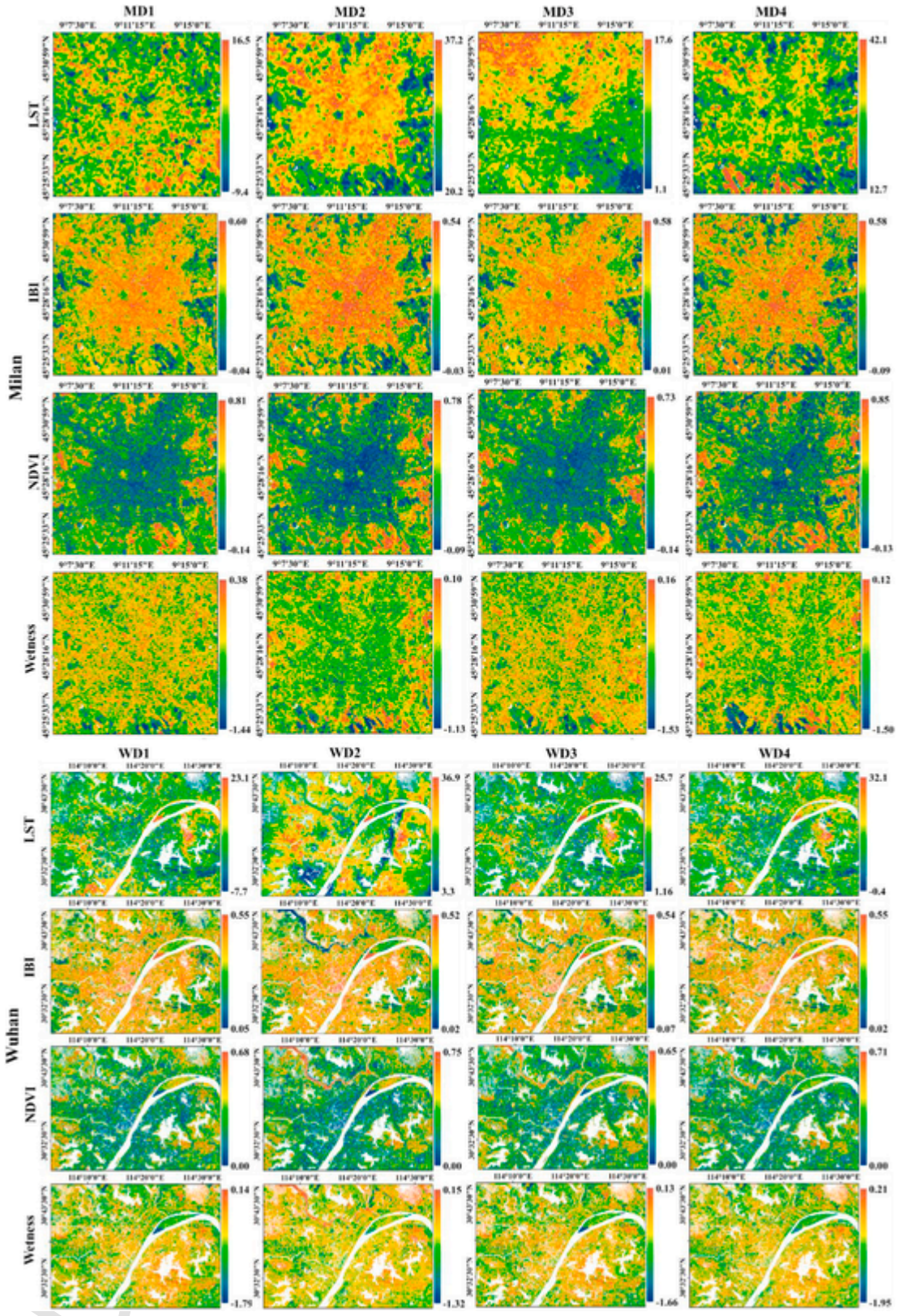

Fig. 3. Surface characteristic maps including heat (LST (°C)), greenness (NDVI), imperviousness and dryness (IBI) and wetness of Milan and Wuhan at pre-lockdown (MD1, MD2, and MD3 for Milan and WD1, WD2 and WD3 for Wuhan) and during the lockdown (MD4 for Milan and WD4 for Wuhan) dates.

Table 4
Mean (SD) of surface characteristics including heat (LST), greenness (NDVI), imperviousness and dryness (IBI) and wetness (Wetness) of Milan and Wuhan cities at pre-lockdown (MD1, MD2, and MD3 for Milan and WD1, WD2 and WD3 for Wuhan) and during the lockdown (MD4 for Milan and WD4 for Wuhan) dates.

		MD1	MD2	MD3	MD4
Milan	LST	9.45	28.77	12.69	31.28
	(°C)	(0.89)	(2.21)	(1.03)	(1.29)
	IBI	0.38	0.32	0.39	0.31
		(0.09)	(0.10)	(0.08)	(0.12)
	NDVI	0.24	0.33	0.21	0.36
		(0.15)	(0.17)	(0.13)	(0.19)
	Wetness	0.02	0.03	0.02	0.02
		(0.01)	(0.02)	(0.01)	(0.02)
		WD1	WD2	WD3	WD4
Wuhan	LST	8.88	20.01	13.15	19.41
	(°C)	(1.53)	(3.44)	(1.63)	(2.02)
	IBI	0.42	0.40	0.42	0.41
		(0.09)	(0.09)	(0.07)	(0.09)
	NDVI	0.19	0.22	0.18	0.19
		(0.11)	(0.11)	(0.10)	(0.11)
	Wetness	0.04	0.036	0.060	0.046
		(0.02)	(0.02)	(0.03)	(0.02)

quently, this amount was less than 24% on WD3 compared to WD1. The implies a significant impact of COVID-19 lockdown on the USES. During the lockdown, the USES significantly improved compared to the similar date last year.

With the significant reduction of human activities in the urban environment due to the COVID-19 lockdown ; in 2020, the USES of these cities in the same climatic and seasonal conditions significantly improved. The average CEEI differences in different lands vary between different dates (Table 8). For Milan, the mean CEEI difference between MD4 and MD2 in built-up, bare soil, and green spaces were −0.18, −0.02 and −0.08, respectively. Also, for Wuhan, the mean difference of CEEI between WD4 and WD2 in these lands were −0.13, −0.06 and −0.05, respectively. This indicates the greatest changes in USES between the COVID-19 lockdown date and the pre-lockdown dates were related to the built-up lands. The r the impervious surface degree (IBI) and the CEEI changes of Milan and Wuhan cities in the COVID-19 lockdown date and its corresponding date last year (MD2 for Milan and WD2 for Wuhan) for the Milan and Wuhan cities were −0.91 and −0.84, respectively. Most changes in USES have been in urban areas with high impervious surface degree.

5. Discussions

Environmentally unfriendly human activities in some urban environments have increased substantially in recent years as reported by many studies such as Firozjaei et al. (2020d), Chen et al. (2019) and Wang et al. (2019). These activities increased environmental consequences such as the formation and increase intensity of urban heat island, increase air and water pollution, degradation of USES, increased thermal discomfort, etc. (Chakraborty et al., 2015; Firozjaei et al., 2020b; Mijani et al., 2020; Nakada and Urban, 2020; Stone, 2008). Given the importance of environmental conditions on the human living quality, quantification of the impact of human activities on various environmental contexts in urban areas is of great importance (Deadman et al., 1993; Hu and Xu, 2018; Xu et al., 2018). Various studies have emphasized the need to reduce destructive human activities in natural and artificial environments to prevent degradation while improving environmental conditions (Firozjaei et al., 2020c; Gaur et al., 2018; Mohajerani et al., 2017; Xu et al., 2018). The prevalence of COVID-19 has created large restrictions for our societies (Velavan and Meyer, 2020). However, the adoption of solutions in the form of social/physical distancing recommendations, the banning of public events, the closure of schools, universities and unnecessary carriers, the closure of external borders and finally lockdown became a mandatory factor in reducing the pressure of human activities on the environment (Nicola et al., 2020).

lockdowns significantly reduced air and water pollution (Berman and Ebisu, 2020; Zambrano-Monserrate et al., 2020), noise pollution (Mandal and Pal, 2020). The rate of USES improvement in the urban environment during the lockdowns compared to pre-lockdown period was highly correlated with the percentage of impervious surface. In previous studies, it was shown that the percentage of impervious surface can be a proper factor to indicate the degree of human activity (Firozjaei et al., 2020d; Li et al., 2018; Sultana and Satyanarayana, 2019). Increasing the impervious surfaces reduces evapotranspiration, increases the LST, increases the urban heat island intensity and reduces the quality of the USES (Firozjaei et al., 2020c). Urban areas with built-up lands have the highest CEEI values due to the low value of greenness and wetness and high value of impervious surface cover, dryness and heat (Figs. 3 and 4 and Table 5). During the lockdown period, due to the decrease in human activities, the heat and dryness of the built-up land area decreased significantly, so that the most improvement in USES was related to urban areas with a high percentage of impervious surface cover. Consequently, the results of this study confirm that reducing human activities in the urban environment can be one of the most effective and useful solutions to improve environmental conditions (Firozjaei et al., 2020d; Xu et al., 2018). Also, COVID-19 lockdowns affected the percentage of vegetation and vegetation health. The effect of lockdowns on plant health is due to a significant reduction in air and water pollution.

In this study, CEEI was used to model the surface ecological status of the urban area. By applying this index, parameters related to PSR framework were used to model the USES (Xu et al., 2019; Yang et al., 2020). The components of this framework include climate responses, environmental states and anthropogenic pressures. Consequently, due to considering more dimensions of environmental conditions, it can have a higher efficiency than other indices such as EI and RSEI in modeling the USES. The advantage of CEEI over RSEI in modeling the USES is the consideration of vegetation health that is not considered in RSEI. CEEI is very fast, simple, scalable, flexible in modeling the USES (Yang et al., 2020).

One of the important challenges in this study is modeling the temporal changes of USES due to changes in human activities (Xu et al., 2018). Modeling the daily USES changes with high spatial resolution in urban environments can be important, versatile and useful. To solve this challenge, the use of satellite imagery with a better temporal resolution than Landsat, such as MODIS images, can be used. However, the spatial resolution of these images is low, which due to the heterogeneity of various characteristics and parameters related to PSR framework in the urban environment, the use of these images can be less informative (Agathangelidis and Cartalis, 2019; Essa et al., 2017). Using downscaling techniques to improve the spatial resolution of satellite images with low spatial resolution can be useful to solve this challenge (Agathangelidis and Cartalis, 2019; Ebrahimy and Azadbakht, 2019; Mukherjee et al., 2014). Also, different effects of climatic conditions such as solar incident angle, wind, air temperature, wind speed, relative humidity, etc. On the USES at different dates can reduce the accuracy of modeling the effect of COVID-19 lockdown on the USES. To overcome this challenge, the use of normalization methods to reduce the impact of climatic conditions on the USES can be useful (Firozjaei et al., 2020a; Weng et al., 2019).

6. Conclusions

The prevalence of COVID-19 had significant negative effects on various aspects of human life in urban and non-urban environments. However, due to reduction of human activities during the lockdown period, the environmental conditions of different parts of the world during this period can be improved. The main purpose of this study was to model the impact of COVID-19 lockdowns on the environment via USES. In this study, CEEI has been used to model and compare the USES during the lockdown and pre-lockdown periods. The results show the significant impact of COVID-19 lockdown on the USES. During the lockdown period, the USES have significantly improved due to the reduction of destructive human activities in the urban environment. The best USES is related to green spaces. Within the COVID-19

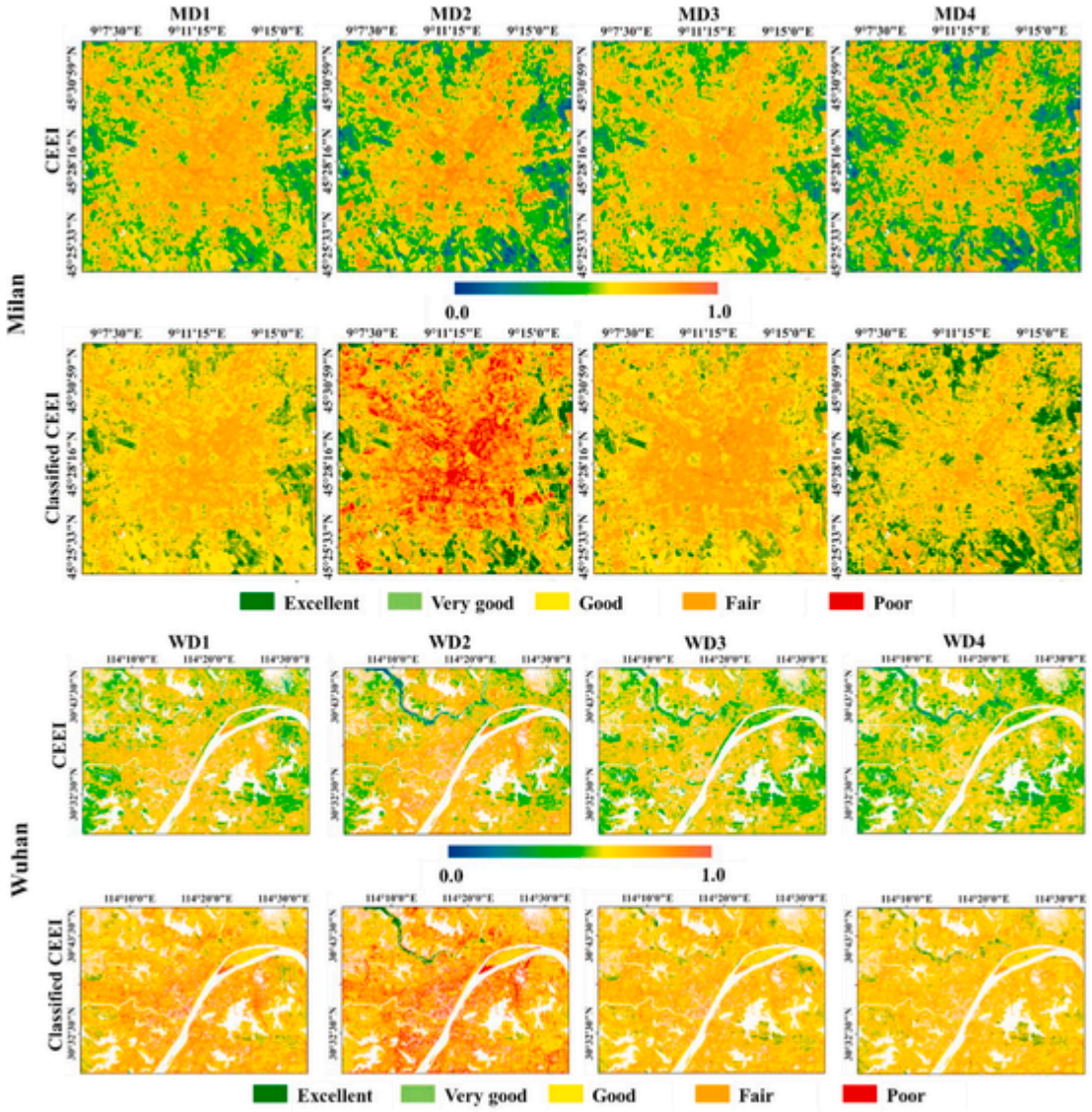

Fig. 4. The USES maps of Milan and Wuhan cities at pre-lockdown (MD1, MD2, and MD3 for Milan and WD1, WD2 and WD3 for Wuhan) and during the lockdown (MD4 for Milan and WD4 for Wuhan) dates.

Table 5
The mean CEEI for land cover in Milan and Wuhan cities at pre-lockdown (MD1, MD2, and MD3 for Milan and WD1, WD2 and WD3 for Wuhan) and during the lockdown (MD4 for Milan and WD4 for Wuhan) dates.

		MD1	MD2	MD3	MD4
Milan	Green space	0.36	0.35	0.39	0.33
	Built-up	0.62	0.76	0.65	0.55
	Bare soil	0.54	0.63	0.56	0.61
		WD1	WD2	WD3	WD4
Wuhan	Green space	0.46	0.48	0.44	0.41
	Built-up	0.67	0.75	0.66	0.59
	Bare soil	0.65	0.72	0.64	0.62

Table 6
The area of USES classes of Milan and Wuhan at pre-lockdown (MD1, MD2, and MD3 for Milan and WD1, WD2 and WD3 for Wuhan) and during the lockdown (MD4 for Milan and WD4 for Wuhan) dates (Km ^{2}).

		MD1	MD2	MD3	MD4
Milan	Excellent	2.59	7.76	2.66	17.30
	Very good	30.54	27.09	21.99	49.06
	Good	96.00	46.04	74.60	82.60
	Fair	67.57	82.41	95.88	47.77
	Poor	0.07	33.48	1.65	0.00
		WD1	WD2	WD3	WD4
Wuhan	Excellent	5.72	10.98	8.34	10.91
	Very good	81.15	51.17	95.41	120.19
	Good	400.26	308.34	455.28	525.56
	Fair	643.05	602.15	645.23	579.75
	Poor	106.71	264.27	32.65	0.51

between the COVID-19 lockdown period and the COVID-19 pre-lockdown period were related to the built-up lands. The r between the percentage of impervious surface cover and CEEI changes between the COVID-19 lockdown date

Table 7
Changes in the USES of Milan and Wuhan cities at pre-lockdown (MD1, MD2, and MD3 for Milan and WD1, WD2 and WD3 for Wuhan) and during the lockdown (MD4 for Milan and WD4 for Wuhan) dates (km ^{2} (%)).

		MD2&MD1	MD4&MD3	MD4&MD2	MD3&MD1
Milan	Improved	15.99 (8.12)	102.03 (51.84)	139.68 (70.97)	8.22 (4.17)
	Unchanged	91.68 (46.58)	89.94 (45.70)	52.25 (26.55)	141.45 (71.87)
	Degraded	89.12 (45.28)	4.81 (2.44)	4.86 (2.46)	47.12 (23.94)
		WD2&WD1	WD4&WD3	WD4&WD2	WD3&WD1
Wuhan	Improved	94.42 (7.63)	244.03 (19.72)	643.33 (52.02)	294.69 (23.82)
	Unchanged	767.06 (62.02)	908.12 (73.43)	519.81 (42.02)	808.04 (65.34)
	Degraded	375.42 (30.35)	84.75 (6.85)	73.76 (5.96)	134.18 (10.84)

Table 8
The mean difference of CEEI of Milan and Wuhan at pre-lockdown (MD1, MD2, and MD3 for Milan and WD1, WD2 and WD3 for Wuhan) and during the lockdown (MD4 for Milan and WD4 for Wuhan) dates.

		MD2&MD1	MD4&MD3	MD4&MD2	MD3&MD1
Milan	Green space	0.00	−0.05	−0.08	0.03
	Built-up	0.14	−0.08	−0.17	0.05
	Bare	0.09	0.04	−0.02	0.02
		WD2&WD1	WD4&WD3	WD4&WD2	WD3&WD1
Wuhan	Veg	0.04	−0.01	−0.05	−0.02
	Built-up	0.03	−0.05	−0.13	−0.03
	Bare	0.06	−0.02	−0.06	−0.04

and its corresponding pre-lockdown date is high. Results of this study show that the effect of human activities on the heterogeneity of spatial distribution of surface ecological status in the urban environment can be higher than the effect of other parameters such as climatic conditions. In future studies, the impact of COVID-19 lockdown on the USES of cities in different climatic conditions can be investigated and the impact of climatic conditions on it needs to be evaluated in more details. Also, the use of techniques to improve spatial and temporal resolution to produce daily USES maps and the impact of human activities on it with high spatial and temporal resolution can be considered in future studies. Despite the fact that COVID-19 pandemic has caused tremendous damages to our society in terms of health and economy, it has brought up thoughts about transferring some of the lessons learned from the pandemic and its lockdowns for climate change and its emerging consequences.

Author contribution statement

Mohammad Karimi Firozjaei: Conceptualization; Data curation; Formal analysis; Investigation; Methodology; Software; Validation; Writing – original draft. Solmaz Fathololomi: Conceptualization; Data curation; Formal analysis; Investigation; Writing – original draft. Majid Kiavarz: Conceptualization; Project administration; Supervision; Writing – review & editing. Seyed Kazem Alavipanah: Conceptualization; Supervision; Validation; Writing – review & editing. Jamal Jokar Arsanjani: Writing – review & editing. Mehdi Homaee: Writing – review & editing.

Declaration of competing interest

The authors declare that they have no known competing financial interests or personal relationships that could have appeared to influence the work reported in this paper.

Acknowledgement

This study was supported by the Iran National Science Foundation (Grant No. 99012975) and Agrohydrology Research Group of Tarbiat Modares University (Grant No. IG-39713).

Appendix A. Supplementary data

Supplementary data to this article can be found online at https://doi.org/10.1016/j.jenvman.2021.112236.

References

[Agathangelidis and Cartalis, 2019] I. Agathangelidis, C. Cartalis, Improving the disaggregation of MODIS land surface temperatures in an urban environment: a statistical downscaling approach using high-resolution emissivity, Int. J. Rem. Sens. 40 (2019) 5261–5286.

[Baig et al., 2014] M.H.A. Baig, L. Zhang, T. Shuai, Q. Tong, Derivation of a tasselled cap transformation based on Landsat 8 at-satellite reflectance, Rem. Sens. Lett. 5 (2014) 423–431.

[Berman and Ebisu, 2020] J.D. Berman, K. Ebisu, Changes in US air pollution during the COVID-19 pandemic, Sci. Total Environ. (2020) 139864.

[Chakraborty and Maity, 2020] T. Chakraborty, P. Maity, COVID-19 outbreak: migration, effects on society, global environment and prevention, Sci. Total Environ. (2020) 138882.

[Chakraborty et al., 2015] S.D. Chakraborty, Y. Kant, D. Mitra, Assessment of land surface temperature and heat fluxes over Delhi using remote sensing data, J. Environ. Manag. 148 (2015) 143–152.

[Chen et al., 2019] S. Chen, D. Hu, M.S. Wong, H. Ren, S. Cao, C. Yu, H.C. Ho, Characterizing spatiotemporal dynamics of anthropogenic heat fluxes: a 20-year case study in Beijing–Tianjin–Hebei region in China, Environ. Pollut. (2019).

[Deadman et al., 1993] P. Deadman, R.D. Brown, H.R. Gimblett, Modelling rural residential settlement patterns with cellular automata, J. Environ. Manag. 37 (1993) 147–160.

[Ebrahimy and Azadbakht, 2019] H. Ebrahimy, M. Azadbakht, Downscaling MODIS land surface temperature over a heterogeneous area: an investigation of machine learning techniques, feature selection, and impacts of mixed pixels, Comput. Geosci. 124 (2019) 93–102.

[Essa et al., 2017] W. Essa, B. Verbeiren, J. van der Kwast, O. Batelaan, Improved DisTrad for downscaling thermal MODIS imagery over urban areas, Rem. Sens. 9 (2017) 1243.

[Firozjaei et al., 2020a] M.K. Firozjaei, S. Fathololoumi, S.K. Alavipanah, M. Kiavarz, A.R. Vaezi, A. Biswas, A new approach for modeling near surface temperature lapse rate based on normalized land surface temperature data, Remote Sens. Environ. 242 (2020a) 111746.

[Firozjaei et al., 2020b] M.K. Firozjaei, S. Fathololoumi, M. Kiavarz, J.J. Arsanjani, S.K. Alavipanah, Modelling surface heat island intensity according to differences of biophysical characteristics: a case study of Amol city, Iran, Ecol. Indicat. 109 (2020b) 105816.

[Firozjaei et al., 2020c] M.K. Firozjaei, S. Fathololoumi, Q. Weng, M. Kiavarz, S.K. Alavipanah, Remotely sensed urban surface ecological index (RSUSEI): an analytical framework for assessing the surface ecological status in urban environments, Rem. Sens. 12 (2020c) 2029.

[Firozjaei et al., 2018] M.K. Firozjaei, M. Kiavarz, S.K. Alavipanah, T. Lakes, S. Qureshi, Monitoring and forecasting heat island intensity through multi-temporal image analysis and cellular automata-Markov chain modelling: a case of Babol city, Iran, Ecol. Indicat. 91 (2018) 155–170.

[Firozjaei et al., 2020d] M.K. Firozjaei, Q. Weng, C. Zhao, M. Kiavarz, L. Lu, S.K. Alavipanah, Surface anthropogenic heat islands in six megacities: an assessment based on a triple-source surface energy balance model, Remote Sens. Environ. 242 (2020d) 111751.

[Foody and Mathur, 2004] G.M. Foody, A. Mathur, Toward intelligent training of supervised image classifications: directing training data acquisition for SVM classification, Remote Sens. Environ. 93 (2004) 107–117.

[Gao et al., 2020] S. Gao, J. Rao, Y. Kang, Y. Liang, J. Kruse, D. Doepfer, A.K. Sethi, J.F.M. Reyes, J. Patz, B.S. Yandell, Mobile Phone Location Data Reveal the Effect and Geographic Variation of Social Distancing on the Spread of the COVID-19 Epidemic, 2020 arXiv preprint arXiv:2004.11430.

[Gaur et al., 2018] A. Gaur, M.K. Eichenbaum, S.P. Simonovic, Analysis and modelling of surface Urban Heat Island in 20 Canadian cities under climate and land-cover change, J. Environ. Manag. 206 (2018) 145–157.

[Hu and Xu, 2018] X. Hu, H. Xu, A new remote sensing index for assessing the spatial heterogeneity in urban ecological quality: a case from Fuzhou City, China, Ecol. Indicat. 89 (2018) 11–21.

[Hughey et al., 2004] K.F. Hughey, R. Cullen, G.N. Kerr, A.J. Cook, Application of the pressure–state–response framework to perceptions reporting of the state of the New Zealand environment, J. Environ. Manag. 70 (2004) 85–93.

[Jiménez-Muñoz et al., 2014] J.C. Jiménez-Muñoz, J.A. Sobrino, D. Skoković, C. Mattar, J. Cristóbal, Land surface temperature retrieval methods from Landsat-8 thermal infrared sensor data, Ieee Geosci Remote S 11 (2014) 1840–1843.

[Lau et al., 2020] H. Lau, V. Khosrawipour, P. Kocbach, A. Mikolajczyk, J. Schubert, J. Bania, T. Khosrawipour, The positive impact of lockdown in Wuhan on containing the COVID-19 outbreak in China, J. Trav. Med. 27 (2020) taaa037.

[Li et al., 2018] H. Li, Y. Zhou, X. Li, L. Meng, X. Wang, S. Wu, S. Sodoudi, A new method to quantify surface urban heat island intensity, Sci. Total Environ. 624 (2018) 262–272.

[Mahato et al., 2020] S. Mahato, S. Pal, K.G. Ghosh, Effect of lockdown amid COVID-19 pandemic on air quality of the megacity Delhi, India, Sci. Total Environ. (2020) 139086.

[Mandal and Pal, 2020] I. Mandal, S. Pal, COVID-19 pandemic persuaded lockdown effects on environment over stone quarrying and crushing areas, Sci. Total Environ. (2020) 139281.

[Mijani et al., 2020] N. Mijani, S.K. Alavipanah, M.K. Firozjaei, J.J. Arsanjani, S. Hamzeh, Q. Weng, Modeling outdoor thermal comfort using satellite imagery: a principle component analysis-based approach, Ecol. Indicat. 117 (2020) 106555.

[Mohajerani et al., 2017] A. Mohajerani, J. Bakaric, T. Jeffrey-Bailey, The urban heat island effect, its causes, and mitigation, with reference to the thermal properties of asphalt concrete, J. Environ. Manag. 197 (2017) 522–538.

[Muhammad et al., 2020] S. Muhammad, X. Long, M. Salman, COVID-19 pandemic and environmental pollution: a blessing in disguise?, Sci. Total Environ. (2020) 138820.

[Mukherjee et al., 2014] S. Mukherjee, P. Joshi, R. Garg, A comparison of different regression models for downscaling Landsat and MODIS land surface temperature images over heterogeneous landscape, Adv. Space Res. 54 (2014) 655–669.

[Nakada and Urban, 2020] L.Y.K. Nakada, R.C. Urban, COVID-19 pandemic: impacts on the air quality during the partial lockdown in São Paulo state, Brazil, Sci. Total Environ. (2020) 139087.

[Nicola et al., 2020] M. Nicola, Z. Alsafi, C. Sohrabi, A. Kerwan, A. Al-Jabir, C. Iosifidis, M. Agha, R. Agha, The socio-economic implications of the coronavirus and COVID-19 pandemic: a review, Int. J. Surg. (2020).

[Otukei and Blaschke, 2010] J.R. Otukei, T. Blaschke, Land cover change assessment using decision trees, support vector machines and maximum likelihood classification algorithms, Int J Appl Earth Obs 12 (2010) S27–S31.

[Qin et al., 2020] C. Qin, L. Zhou, Z. Hu, S. Zhang, S. Yang, Y. Tao, C. Xie, K. Ma, K. Shang, W. Wang, Dysregulation of immune response in patients with COVID-19 in Wuhan, China, Clin. Infect. Dis. (2020).

[Robinson et al., 2017] N.P. Robinson, B.W. Allred, M.O. Jones, A. Moreno, J.S. Kimball, D.E. Naugle, T.A. Erickson, A.D. Richardson, A dynamic Landsat derived normalized difference vegetation index (NDVI) product for the conterminous United States, Rem. Sens. 9 (2017) 863.

[Sobrino et al., 2008] J.A. Sobrino, J.C. Jiménez-Muñoz, G. Sòria, M. Romaguera, L. Guanter, J. Moreno, A. Plaza, P. Martínez, Land surface emissivity retrieval from different VNIR and TIR sensors, Ieee T Geosci Remote 46 (2008) 316–327.

[Stone, 2008] B. Stone, Urban sprawl and air quality in large US cities, J. Environ. Manag. 86 (2008) 688–698.

[Sultana and Satyanarayana, 2018] S. Sultana, A. Satyanarayana, Impact of urbanisation on urban heat island intensity during summer and winter over Indian metropolitan cities, Environ. Monit. Assess. 191 (2019) 789.

[Tobías et al., 2020] A. Tobías, C. Carnerero, C. Reche, J. Massagué, M. Via, M.C. Minguillón, A. Alastuey, X. Querol, Changes in air quality during the lockdown in Barcelona (Spain) one month into the SARS-CoV-2 epidemic, Sci. Total Environ. (2020) 138540.

[Velavan and Meyer, 2020] T.P. Velavan, C.G. Meyer, The COVID-19 epidemic, Trop. Med. Int. Health 25 (2020) 278.

[Wang et al., 2019] S. Wang, D. Hu, S. Chen, C. Yu, A partition modeling for anthropogenic heat flux mapping in China, Rem. Sens. 11 (2019) 1132.

[Weng, 2009] Q. Weng, Thermal infrared remote sensing for urban climate and environmental studies: methods, applications, and trends, Isprs J Photogramm 64 (2009) 335–344.

[Weng et al., 2019] Q. Weng, M.K. Firozjaei, M. Kiavarz, S.K. Alavipanah, S. Hamzeh, Normalizing land surface temperature for environmental parameters in mountainous and urban areas of a cold semi-arid climate, Sci. Total Environ. 650 (2019) 515–529.

Who https://www.who.int/emergencies/diseases/novel-coronavirus-20192020

[Xiao and Weng, 2007] H. Xiao, Q. Weng, The impact of land use and land cover changes on land surface temperature in a karst area of China, J. Environ. Manag. 85 (2007) 245–257.

[Xu, 2008] H. Xu, A new index for delineating built-up land features in satellite imagery, Int. J. Rem. Sens. 29 (2008) 4269–4276.

[Xu et al., 2018] H. Xu, M. Wang, T. Shi, H. Guan, C. Fang, Z. Lin, Prediction of ecological effects of potential population and impervious surface increases using a remote sensing based ecological index (RSEI), Ecol. Indicat. 93 (2018) 730–740.

[Xu et al., 2019] H. Xu, Y. Wang, H. Guan, T. Shi, X. Hu, Detecting ecological changes with a remote sensing based ecological index (RSEI) produced time series and change vector analysis, Rem. Sens. 11 (2019) 2345.

[Yang et al., 2020] C. Yang, C. Zhang, Q. Li, H. Liu, W. Gao, T. Shi, X. Liu, G. Wu, Rapid urbanization and policy variation greatly drive ecological quality evolution in Guangdong-Hong Kong-Macau Greater Bay Area of China: a remote sensing perspective, Ecol. Indicat. 115 (2020) 106373.

[Zambrano-Monserrate et al., 2020] M.A. Zambrano-Monserrate, M.A. Ruano, L. Sanchez-Alcalde, Indirect effects of COVID-19 on the environment, Sci. Total Environ. (2020) 138813.